Received: 8 January 2020 | Revised: 24 February 2020 | Accepted: 25 March 2020

DOI: 10.1111/ina.12672

WILEY

ORIGINAL ARTICLE

Performance evaluation of ductless personalized ventilation in comparison with desk fans using numerical simulations

Hayder Alsaad | Conrad Voelker

Department of Building Physics, Bauhaus-Universität Weimar, Weimar, Germany

Correspondence
Hayder Alsaad, Department of Building Physics, Bauhaus-Universität Weimar, Coudraystrasse 11A, Weimar 99423, Germany.
Email: hayder.alsaad@uni-weimar.de

Funding information
Deutscher Akademischer Austauschdienst, Grant/Award Number: Programme ID: 57129429

Abstract

The performance of ductless personalized ventilation (DPV) was compared to the performance of a typical desk fan since they are both stand-alone systems that allow the users to personalize their indoor environment. The two systems were evaluated using a validated computational fluid dynamics (CFD) model of an office room occupied by two users. To investigate the impact of DPV and the fan on the inhaled air quality, two types of contamination sources were modeled in the domain: an active source and a passive source. Additionally, the influence of the compared systems on thermal comfort was assessed using the coupling of CFD with the comfort model developed by the University of California, Berkeley (UCB model). Results indicated that DPV performed generally better than the desk fan. It provided better thermal comfort and showed a superior performance in removing the exhaled contaminants. However, the desk fan performed better in removing the contaminants emitted from a passive source near the floor level. This indicates that the performance of DPV and desk fans depends highly on the location of the contamination source. Moreover, the simulations showed that both systems increased the spread of exhaled contamination when used by the source occupant.

KEYWORDS

computational fluid dynamics, desk fan, ductless personalized ventilation, IAQ, thermal comfort, thermal sensation

1 | INTRODUCTION

The quality of the indoor environment is a key factor in determining the wellness and productivity of occupants. Therefore, the built environment is often equipped with mechanical systems to regulate the indoor temperature, introduce fresh air from the outdoors, and remove contaminants from the rooms. Room contaminants are generated from the occupants in the form of exhaled viruses and bacteria or in the form of dermally emitted bioeffluents and body odors.[1,2] Another source of room contamination is volatile organic compounds (VOCs) emitted into the space from finishing material and furniture.[3] Additionally, electronic devices (such as personal computers) can generate contamination as well.[4] Low air quality can lead to health issues such as headaches and sick building syndrome (SBS), which decrease the productivity of occupants and affect their ability to concentrate.[5,6]

In order to improve the quality of the indoor environment, personalized ventilation has been suggested in combination with common total-volume systems.[7] Personalized ventilation (PV) is a system that provides fresh air directly to the occupant's breathing zone. It

allows individual control over air velocity, direction, and possibly temperature as well.[1] Numerous studies reported in the literature indicate that PV in combination with background total-volume systems can significantly improve the indoor environment.[8,9] However, even though PV offers numerous advantages, PV can be a significant limitation when designing a space as it is typically connected to a duct supplying fresh tempered air from the outdoors. This considerably increases the ductwork of a project, restricts the arrangement of furniture in the room, and affects its aesthetics. Therefore, a ductless personalized ventilation system (DPV) has been suggested.[10] "Ductless" personalized ventilation is, as the name suggests, a self-standing system that is not connected to a duct that supplies air from the outdoors. It is used in combination with displacement ventilation (DV) because DV creates vertical air stratification in which the cool fresh air is concentrated at the lower layer of the air and the warm polluted air is concentrated at the upper layer of the air due to buoyancy forces generated by the heat sources in the room.[11] DPV transports the cool fresh air from the lower part of the room and delivers it directly into the occupant's breathing zone. DPV is typically a desk-mounted system; it consists of an air intake to suck the air from the lower part of the room, a short duct system with an embedded electric axial fan, and a supply diffuser. Ductless personalized ventilation is not as widely examined in the literature as regular ducted personalized ventilation. However, published studies indicate that using DPV in combination with DV improves perceived indoor air quality especially in elevated indoor air temperatures.

Dalewski et al[10,12] investigated the human response to DPV compared to reference cases with no DPV (DV or MV alone). The subjects indicated that DPV resulted in better air quality and thermal comfort in comparison with having DV alone. Their results showed that DPV at elevated room air temperatures achieved the same level of percentage dissatisfied as DV or MV alone at a lower room air temperature. Further experimental studies were conducted by Halvoňová and Melikov[13] to evaluate the influence of partitions and workstation layout on the performance of DPV. The obtained findings showed that the office layout had a clear effect on the inhaled air quality. This can be explained due to changing the location of the contamination source in each tested setup. Another study was conducted by the same authors[14] to study the effects of disturbance caused by a walking person on the performance of DPV using empirical measurements. It showed that a walking person caused mixing of cool fresh air supplied by DV at floor level with polluted warmer air at the higher levels of air, hence reducing air quality. However, even when a walking person disturbed vertical air stratification generated by DV, DPV still achieved better results compared to the cases in which DV was used with no DPV.

Since DPV offers numerous advantages in improving the indoor environment in rooms equipped with DV, the number of studies that investigates its performance has remarkably increased in the past years. However, DPV remains unintegrated into the market due to reasons connected to its cost and practicality despite its independency from the building automation system. When a personalized comfort system is needed in a room, axial fans are commonly implemented to improve the built environment even though they only address thermal comfort without improving the contaminants' concentration levels in the room. Axial fans are a common mean of improving thermal comfort in hot environments by increasing air movement.[15] Unlike the flow of PV, which has a low initial turbulence and a uniform velocity field across the PV opening,[1] the axial fans supply a "choppy" swirling flow with high turbulence intensity over a large target area.[16] Early research about the impact of fans on thermal comfort dates back to the mid-seventies by Rohles et al[17] It was found the effective room air temperature could be stretched to 29°C at 1 m/s air velocity. Further research indicated that at 28°C room temperature and about 1 m/s air velocity, up to 80% of the occupants could reach thermal comfort.[18] Other studies suggest that air velocity can be up to 1.4 m/s to achieve thermal comfort for 80% of the subjects at 29°C ambient temperature and 1.2 met metabolic rate, or at 31°C temperature and 1 met metabolic rate.[19] Yang et al[20] found that the lower the room temperature and the shorter the distance between the stand fan and its target, the higher the cooling efficiency in relation to power consumption. Schiavon et al[21] reported that by using stand fans, the test subjects experienced similar or improved thermal comfort, perceived air quality, and SBS symptoms at room temperature of 26 and 29°C when having individually controlled fans in comparison with a room temperature of 23°C without fans. Similar results were reported in the work of Zhai et al[22] which suggests the possibility of increasing the room air temperature when air movement is induced by ceiling fans. They report that at 80% relative humidity, more than 80% of the surveyed subjects found the thermal environment acceptable with ceiling fans at 30°C room temperature or at 26°C without ceiling fans.

Although multiple studies in the literature investigated the performance of DPV and axial fans, the two systems have not been extensively compared to each other even though both of them are stand-alone systems that induce air movement within the room. The systems should be compared to address the question of whether DPV is really better than a simple inexpensive fan. The present study investigates a detailed office setup with multiple heat and contamination sources utilizing CFD simulations to compare the inhaled air quality and thermal comfort provided by DPV and desk fans. However, it is important to point out that a direct comparison

Practical Implications

- This study provides an insight for designer and developers about the performance of the ductless personalized ventilation and desk fans under various boundary conditions.
- It also provides information for the occupants about the systems' potential for improving both thermal comfort and indoor air quality in relation to the location of contamination sources in rooms ventilated with displacement ventilation during the summer season.

between the two systems is difficult since the nature of the supplied airflow is completely different regarding the flow pattern, turbulence intensity, and distribution of the velocity across the section of the system outlet. Therefore, this study assumes that the desk fan supplies the same flow pattern as DPV. In this case, the main difference between DPV and desk fans is the location from where the air is moved. While DPV takes air from the floor level, the fan moves the air within the head height.

2 | METHODS

The performance of the systems was evaluated using steady-state CFD simulations conducted by the commercial code Ansys Fluent. CFD was selected as a research tool as it is a fast affordable approach that can simulate the complex attributes of the indoor airflow.[23] The performance of DPV and the desk fan was assessed in comparison with a reference case where DV was used with no personalized system in the room. Thus, three cases were compared: DV, DPV, and fan. Before conducting the simulations, the numerical model was first validated against empirical measurements conducted in a climate chamber equipped with a thermal manikin. The validation work included testing multiple combinations of turbulence models, pressure interpolation schemes, and solver settings. Figure 1 presents the measured and simulated air temperature and velocity at the manikin's face using the validated model under four combinations of room set-point temperature and target air velocity at the face. The error bars indicate the standard deviation of the measurements, which corresponds to the measured fluctuations over time. An extensive description of the validation work and its results could be found in Alsaad and Voelker.[24] The implemented settings of the validated model are reported in Section 2.4.

Skin temperature, thermal sensation, and comfort were evaluated using the coupling of CFD and the University of California, Berkeley (UCB), comfort model. The UCB model is a mathematical model that can simulate numerous occupants' responses such as skin temperature, thermal sensation, and thermal comfort. Skin temperature is determined in the model using an advanced thermoregulation model developed and validated by Huizenga et al[25] This thermoregulation model accounts for complex physiological mechanisms such as vasodilation, vasoconstriction, sweating, and metabolic rate. This function was implemented in this study to determine the skin temperature of the occupants' body parts as a boundary condition in the CFD model. Thermal comfort and sensation are evaluated in the UCB model based on Zhang's model,[26] which allows assessing comfort and sensation in the non-uniform thermal environments typically generated by personalized systems. It can evaluate the thermal condition of the whole body as well as locally for 16 body segments.[26] The details of the coupling and setup of the UCB model are reported in Section 2.4.

2.1 | Geometry and configuration

The systems were assessed in a simulated office room geometry with the dimensions of 3 × 3 × 2.44 m, which corresponds to the same size of the climate chamber in which the model validation study was conducted. As shown in Figure 2, air was supplied to the domain through a semi-circular wall-mounted displacement ventilation supply air terminal; the exhaust outlet was located at the center of the ceiling. Four lighting fixtures were mounted on the ceiling around the exhaust outlet. Two workstations were located at the center of the office; each workstation was equipped with a computer case and two computer screens. Two occupants were simulated using a 3d scanned geometry of the thermal manikin; the occupants were in the seated position, yet the geometry of the chair was not modeled to simplify the model. The heat load of each heat source was defined in the solver according to their typical values reported in the ASHRAE standard[27] (occupants = 2 × 70 W, lighting fixtures = 4 × 20 W, computer cases = 2 × 75 W, computer screens = 4 × 32 W). The total cooling load in the simulated office was 55.3 W/m^2. DPV outlet was located in front of the occupants with a diameter of 18 cm

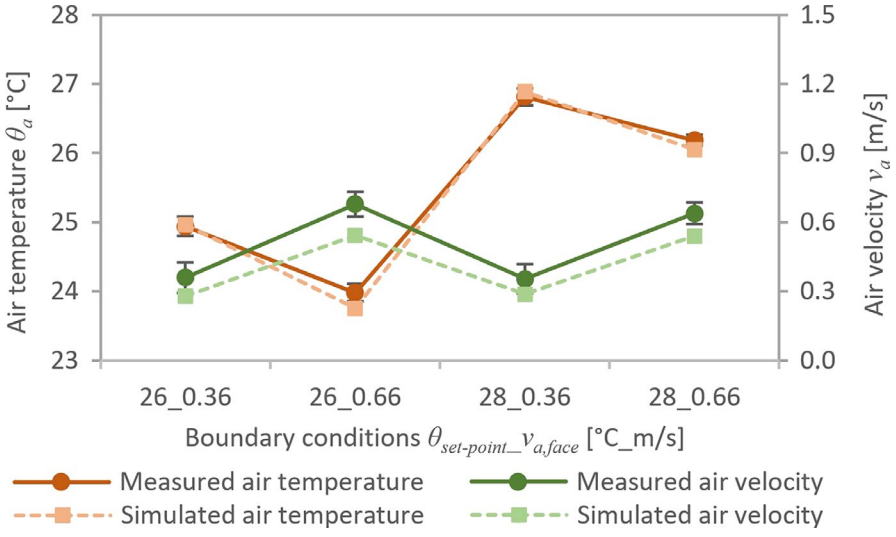

FIGURE 1 Measured and simulated air temperature and velocity at the manikin's face during four combinations of boundary conditions

based on the round moveable panel proposed by Bolashikov et al[28]; the geometry of the desk fan was modeled with the same diameter to allow a direct comparison. The heat generated by the electric fan embedded in DPV and the desk fans was not simulated in this study.

Both occupant geometries had two nostril openings; both openings were directed 45° below the horizontal direction; the intervening angle between the two nostrils was 30°.[29,30] Since the simulations were conducted under steady state, the transient respiratory process was replaced with a continuous inhalation and continuous exhalation according to the findings of Pantelic et al,[31] which indicated that both realistic and continuous (unrealistic) breathing processes resulted in the same measured contamination concentration in the manikin's breathing zone. Hence, in this study, one occupant constantly exhaled air through the nose with an exhaled air temperature of 34°C and a fixed pulmonary flow rate of 6 L/min,[32,33] while the other occupant constantly inhaled air through the nose with the same rate.

The exhaled air was marked with sulfur hexafluoride (SF_6) to simulate infectious polluted air with droplet nuclei smaller than 5-10 μm.[34,35] Therefore, the exhaling occupant is denoted as the "polluting occupant," while the inhaling occupant is denoted as the "exposed occupant." Accordingly, the workstation of the exhaling occupant is denoted as the "polluting workstation," while the workstation of the inhaling occupant is denoted as the "exposed workstation." Furthermore, nitrous oxide (N_2O) was released into the domain from the top of a trash bin located by the wall (Figure 2) to simulate a passive contamination source.

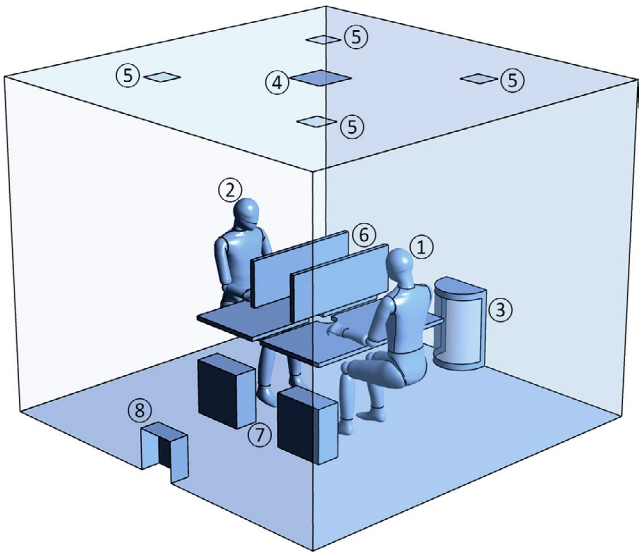

FIGURE 2 The configuration of the simulated reference case: (1) exhaling "polluting" occupant, (2) inhaling "exposed" occupant, (3) displacement ventilation air terminal, (4) exhaust outlet, (5) ceiling lights, (6) screens (two per desk), (7) computer cases, and (8) trash bin

2.2 | Mesh generation and properties

The mesh was generated using the meshing tool in ANSYS Workbench according to the settings recommended by the model validation study in Alsaad and Voelker.[24] Test simulations were conducted to proof the independency of the solution from the size of the cells by refining the mesh systematically until additional refinements yielded no significant changes in the simulation results. The implemented mesh was generated using a maximum cell size of 0.06 m with a curvature normal angle of 18° and a minimum of three cells across gaps. An advanced size function was used to generate the mesh based on proximity and curvature. Local sizing functions were imposed to refine the mesh on critical surfaces as follows: DV inlet and exhaust outlet = 0.005 m; nostrils = 0.001 m; and lighting fixtures, computer cases, and trash top = 0.02 m. The central region of the domain containing the breathing zones of the occupant geometries was refined using a 2 × 0.75 × 0.38 m sizing region to accurately capture the contaminants that transport from and into the breathing zone of the two occupants. The elements' size in this domain was set to 0.014 m. The portion of the computer screens that was out of this domain was also sized to 0.014 m using a surface sizing function. All sizing functions were set to soft behavior and a growth rate of 20%.

Mesh inflation layers were created around the occupants, walls, and surfaces in the model to accurately capture the flow properties in the boundary regions. Four inflation layers were created using the smooth transition method with a ratio of 0.272 and a growth rate of 20%. The average y + value for the first layer of cells near the occupants' surface was < 1, which is necessary to resolve the wall-bounded turbulent flows at the cell layers next to the surface (where large gradients are expected) without using a wall function for near-wall turbulence modeling.[36-38] These operations led to a

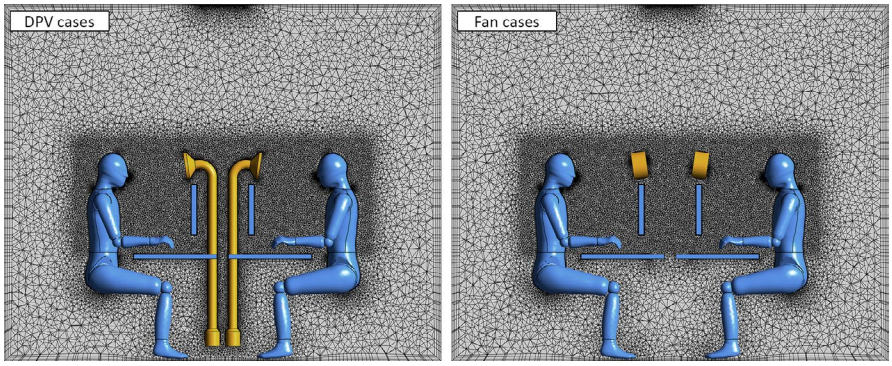

FIGURE 3 The generated mesh of the DPV and desk fan cases. The view plane is located at the center of occupant geometry (between the legs)

final mesh of ~ 6.48 million unstructured tetrahedral cells. The mesh properties listed above were used during all three simulated variations (DV reference cases, DPV cases, and desk fan cases). As shown in Figure 3, the openings of the personalized systems were located within the sizing region. Therefore, no sizing function was imposed on those surfaces. A surface sizing function was used to limit the size of elements at the DPV intake to 0.014 m. Furthermore, 4 inflation layers were created on the walls of the personalized systems using the smooth transition method with a ratio of 0.272 and a growth rate of 20% as well.

2.3 | Boundary conditions

The evaluated systems were compared under different combinations of ventilation flow rates, room air temperature, personalized flow rate, and operation modes. The room ventilation flow rate was calculated according to the ASHRAE procedure outlined by Chen and Glicksman[39] and rounded to $\dot{V}_{DV}$ = 60 L/s. A further ventilation flow rate of $\dot{V}_{DV}$ = 75 L/s was simulated as well to investigate the influence of a larger amount of supplied fresh air on the performance of the studied systems. Thus, the compared systems were evaluated under an air change rate of 10 and 12 h. The evaluated systems were compared under two room air temperature set points (taken at 1.1 m from the floor): $\theta_{set\text{-}point}$ = 26 and 29°C. A set point of 26°C corresponds to the recommended value for summer in office spaces for buildings in Category II (−0.5 < PMV < +0.5; PPD < 10%). [40] On the other hand, the set point of 29°C was selected to investigate the influence of the systems on thermal comfort at an elevated indoor air temperature. Thus, the systems were tested under both comfortable and uncomfortable thermal environments.

Each personalized system was evaluated under two personalized flow rates: 10 and 20 L/s, which corresponded to a target velocity at the face of 0.34 and 0.54 m/s, respectively, according to the recommendations of Bolashikov et al[28] Moreover, two operation patterns were simulated: (a) the personalized system is switched on at both workstations, and (b) the personalized system of the "polluting occupant" is switched off, while the system of the "exposed occupant" is switched on. The second operation pattern was investigated only for the cases with room ventilation flow rate of 75 L/s. Table 1 summarizes the simulated cases and the investigated boundary conditions. In order to facilitate following the compared simulation cases, a naming system was used to express the implemented personalized system and the boundary conditions. The name of each simulation case consists of: (simulated system_room ventilation flow rate_room air temperature). The flow rate of the simulated system was written in subscript after the system's name, while the prefixes "2x" and "1x" were added to the case names to indicate whether the personalized system is switched on at both workstations or switched on at only one workstation (at the exposed occupant's workstation) while the other personalized system is switched off (at the polluting occupant's workstation). For example, a case named $2xFan_{20}$_60_26 corresponds to a simulation case where the desk fan is switched on at both workstations with a flow rate of $\dot{V}_{Fan}$ = 20 L/s, a room ventilation flow rate of $\dot{V}_{DV}$ = 60 L/s, and a room air temperature set point of $\theta_{set\text{-}point}$ = 26°C. Finally, in the CFD images in the following sections, the "polluting occupant" and the "exposed occupant" are marked with P and E, respectively, to make them easier to identify.

2.4 | Numerical model settings

Based on the validation work of the numerical model,[24] the simulations were conducted using the realizable k-ε turbulence model with enhanced wall treatment and full buoyancy effects. Buoyancy effects were simulated using the incompressible ideal gas law for air density. Species transport model was used to calculate tracer gas concentrations in the domain. Coupled pressure-velocity scheme was used along with PRESTO spatial pressure discretization scheme and second-order upwind discretization scheme to solve the equations of momentum, turbulent kinetic energy and dissipation rate, energy, and species transport. Initial simulations indicated convergence difficulties due to the unsteady features of buoyancy yielded by the displacement ventilation system.[37,38] To resolve these issues, the pseudo-transient implicit under-relaxation method was used to solve time-dependent partial differential equations in steady-state simulations.[41] Thus, pseudo-transient allows simulating the transient behavior of natural convection within a steady-state solution. Radiant heat exchange was not simulated in this study since the

TABLE 1 A summary of the simulated systems and boundary conditions

Parameter	Details
Simulated systems	DV (reference case with only displacement ventilation, no personalized system) DPV (ductless personalized ventilation in conjunction with displacement ventilation) Fan (desk fan in conjunction with displacement ventilation)
Operation mode	System switched on at both desks System switched on at the exposed desk only
Personalized flow rate	$\dot{V}_{DPV} = \dot{V}_{Fan}$ = 10 and 20 L/s
Room ventilation rate	$\dot{V}_{DV}$ = 60 and 75 L/s
Room air temperature	$\theta_{set\text{-}point}$ = 26 and 29°C

domain has no large radiant asymmetries. With the absence of such asymmetries, excluding radiant heat transfer from the simulations is a common practice in the literature as it has no direct impact on the airflow in the room.[24,42]

In the numerical domain, the computer cases, screens, and lighting fixtures were defined as fixed heat flux boundary condition; the room walls, floor, ceiling, and the surfaces of the desks and the trash bin were defined as adiabatic surfaces. The DV supply inlet and the exhaling nostrils were defined as velocity inlets. The inhaling nostrils were defined as a velocity inlet with a negative velocity magnitude to define the velocity of the flow exiting the domain. The room exhaust outlet was modeled as a pressure outlet with 0 Pa gauge pressure.

The geometry of each occupant was divided into 16 segments and defined in the solver as a fixed temperature boundary condition. Even though minor changes in the surface temperature of the occupant may have a relatively small influence on the inhaled air quality,[43] the surface temperature plays an important role in determining the thermal state.[26] Therefore, it is necessary to define the body surface temperature accurately in the numerical model. The surface temperature of each body segment was determined in this study through the coupling of CFD and the UCB comfort model. In order to determine the surface temperature, initial CFD simulations were conducted with a uniform surface temperature for all the body segments of 34°C.[44] The resulted air temperature and velocity surrounding each body segment were input into the UCB model to calculate the surface temperature of each body segment. Subsequently, the calculated surface temperatures were input into the CFD model. By using this approach, even though the occupants were geometrically naked and the office chair geometry was not modeled, the body segments' surface had a temperature of a dressed occupant wearing typical summer clothing (clothing level = 0.5 clo) and seated on an office chair. The default Stolwijk body model was used[45]; the metabolic rate was set to a standard value of 1.1 met to simulate a seated person doing light tasks.[27] The relative humidity was left to its default value of 50%. The UCB simulations were conducted in this study using a time constant model with a simulation time of t = 300 min to ensure reaching steady state. Finally, the same UCB model settings were used to evaluate thermal sensation and comfort by importing the final results of the CFD simulations into the UCB model. The coupling conducted in this study was manual; advanced automated coupling such as in Voelker and Alsaad[46] was not implemented.

3 | RESULTS

3.1 | Inhaled air quality

The inhaled air quality was assessed according to the simulated tracer gas concentration inhaled by the exposed occupant. However, it is important to point out that this approach actually evaluates "air cleanness" rather than "air quality," as indoor air quality is determined by three parameters: air temperature, humidity, and the pollutants' concentration in the inhaled air.[47] However, evaluating air cleanness as an indicator of indoor air quality is widely used in literature, and therefore, it is used in this study as well. The contaminants' distribution was evaluated in this study by comparing the mass fraction of each tracer gas w_j [-], which is defined as the ratio of the mass of a certain tracer gas m_j [mg] to the mass of the total mixture m_t. Thus, high mass fraction values indicate high tracer gas concentrations. In other words, the lower the mass fraction, the better the indoor air quality.

Figure 4 illustrates the SF_6 mass fraction inhaled by the exposed occupant when both workstations had a switched-on DPV or desk fan. It shows that both DPV and the fan increased SF_6 concentration inhaled by the exposed occupant, whereas the reference cases with DV alone delivered a lower SF_6 mass fraction. This is due to the thermal plumes from the computer screens, which were creating an "air shield" protecting the exposed occupant from the exhaled contamination from the polluting occupant, thus resulting in a low inhaled SF_6 concentration during the DV cases. Yet, when DPV or the fan was switched on at both desks, the exhaled SF_6 molecules were mixed into the space because of the air momentum directed at the exhaling occupant's face. Thus, the SF_6 concentration inhaled by the exposed occupant was higher.

During the DV cases, case DV_75_26 achieved the best removal of SF_6 from the air inhaled by the exposed occupant, where the SF_6 mass fraction was $w_{j,SF6} = 0.08 \times 10^{-5}$. On the other hand, case DV_60_29 achieved the least level of SF_6 removal at the same location ($w_{j,SF6} = 0.17 \times 10^{-5}$). To recap, the high DV flow rate at a relatively low temperature achieved the best results, while the low DV flow rate at a higher temperature achieved the lowest SF_6 removal. This is because that larger amount of fresh air supplied by the high DV flow rate can remove more contamination. Additionally, lower room air temperature leads to stronger buoyancy-induced flow around the computer screens and the body of the exposed occupant, thus protecting the exposed occupant from SF_6 exhaled by the polluting occupant, and transporting SF_6 molecules toward the exhaust outlet. This strong buoyancy-induced flow is resulted from

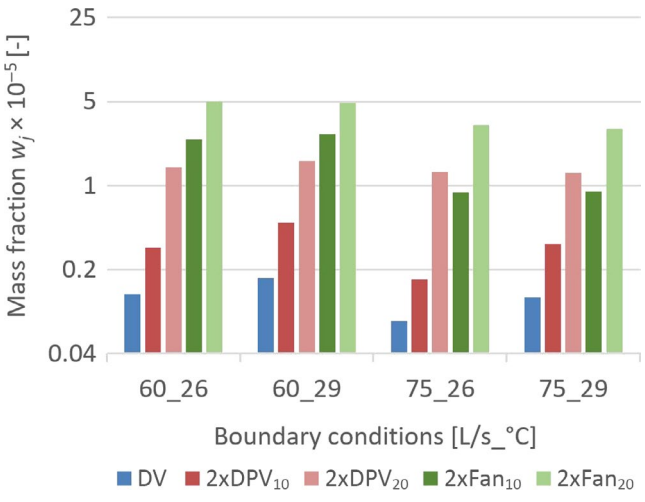

FIGURE 4 SF_6 mass fraction inhaled by the exposed occupant, DPV and the fan are switched on at both workstations

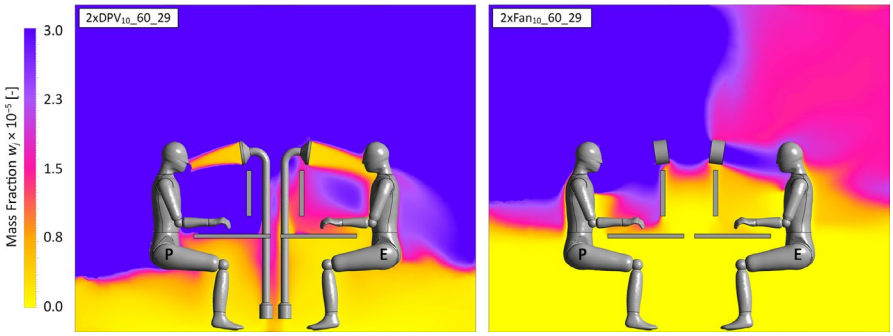

FIGURE 5 SF_6 mass fraction during the $2xDPV_{10}$_60_29 and $2xFan_{10}$_60_29 cases

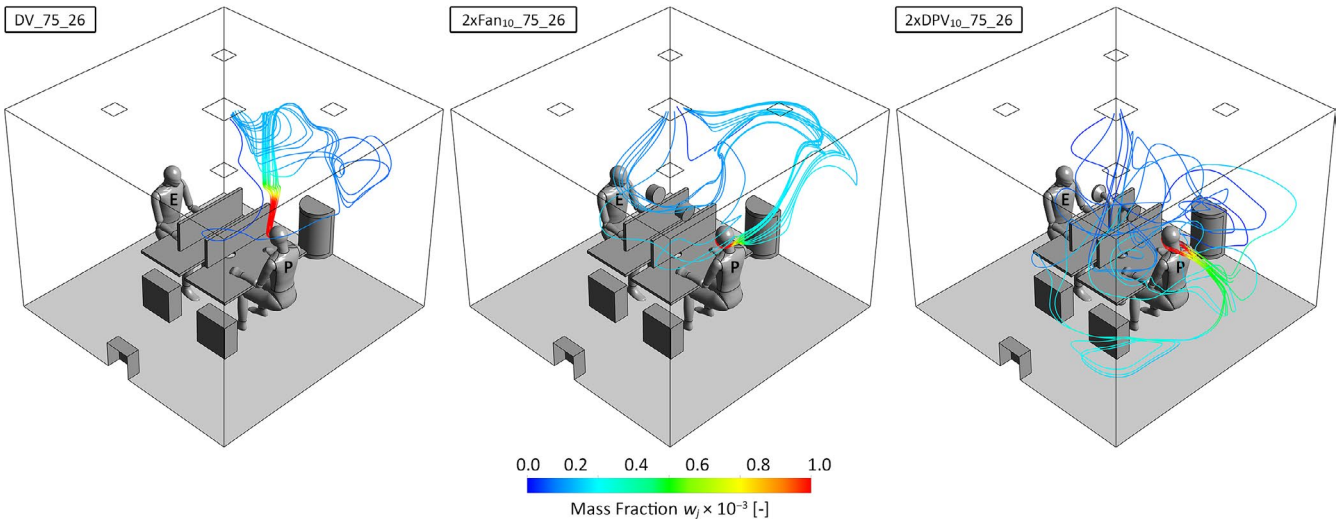

FIGURE 6 SF_6 mass fraction in the flow streamlines originating from the exhaling occupant's nostrils during the 75_26 cases

the larger difference between the surface temperature and air temperature, hence higher Rayleigh number. Thus, the higher the temperature difference, the higher the air velocity in the boundary layer surrounding the heat sources.[48]

However, when comparing the performance of DPV and the fan, the fan cases resulted in a higher concentration of inhaled SF_6. During DPV_{10} cases, the highest level of inhaled SF_6 mass fraction was 0.49×10^{-5} during the $2xDPV_{10}$_60_29 case. On the other hand, Fan_{10} cases resulted in the highest SF_6 mass fraction (2.69 during the $2xFan_{10}$_60_29 case). This difference in DPV and desk fan performance is due to the source of air transported by the system into the breathing zone. While DPV was transporting clean air from the floor level to breathing zone of the exposed occupant, the fan was basically sucking SF_6 from the polluting occupant's workstation, where SF_6 concentration is at its maximum level between the ascending thermal plumes of the polluting occupant and his/her computer screens. The sucked SF_6 gas was moved directly toward the exposed occupant's breathing zone (Figure 5). This effect was even higher when the flow rate of the fan was increased to 20 L/s (ie, Fan_{20} cases) due to the increased amount of SF_6 that was moved toward the exposed occupant. In Fan_{20} cases, the inhaled SF_6 mass fraction was as high as 5.02×10^{-5} during the $2xFan_{20}$_60_26 case. Alternatively, the same boundary conditions yielded an inhaled SF_6 mass fraction of 1.42×10^{-5} during the $2xDPV_{20}$ case. This indicates that increasing the personalized flow rate from 10 L/s to 20 L/s reduces the performance difference of DPV and the fan when the systems were used at both workstations.

Figure 6 illustrates the impact of DPV and the fan on the exhaled SF_6 gas; it shows that both systems assisted the diffusion of the gas in the room in comparison with the reference case in which the exhaled heated gas rose toward the exhaust outlet with smaller diffusion into the room air. Thus, when the DPV or the fan at the polluting occupant's workstation was switched off, the spread of exhaled contaminants is reduced significantly.

Figure 7 compares the performance of the systems when the system was switched on at a single workstation or at both workstations. It indicates that while the fan scenarios increased the inhaled SF_6 concentration, the DPV scenarios decreased SF_6 inhaled concentration compared to the reference cases. The $1xDPV_{10}$_75_26 cases resulted in the lowest inhaled SF_6 concentration ($w_{j,SF6} = 0.89 \times 10^{-7}$), which is eight times smaller than what it was during the DV_75_26 reference case. Thus, DPV system switched on only at the exposed workstation (1xDPV cases) improved the inhaled air quality. On the contrary, having only one desk fan switched on resulted in a higher inhaled SF_6 concentration compared to having both of the fans switched on. This is because the polluting occupant's fan diffused SF_6 into the rest of the room. Thus, the SF_6 concentration "sucked" by the exposed occupant's fan was smaller when both fan systems

were switched on. The lowest inhaled SF_6 mass fraction during the 1xFan cases was $w_{j,SF6} = 1.6 \times 10^{-5}$, which is about 21 times higher than in the reference case.

Increasing the flow rate of DPV to $\dot{V}_{DPV} = 20$ L/s ($1xDPV_{20}$ cases) did not improve the DPV performance compared to the $1xDPV_{10}$ cases. This is due to increased mixing of SF_6 with the transported air at the DPV intake. However, the $1xDPV_{20}$ cases still achieved improved inhaled air quality compared to the DV reference cases. The $1xFan_{20}$ cases also increased the inhaled SF_6 concentration compared to the $1xFan_{10}$ cases due to the larger amount of transported SF_6 toward the exposed occupant.

Different results are observed when examining the spread of N_2O, which was emitted into the domain from the top of the trash bin. This contamination source was located 0.3 m from the floor releasing unheated N_2O molecules into the room (passive source). Since N_2O is about 1.6 times heavier than air, the emitted N_2O was concentrated at the lower part of the room, where it was mixed with the air supplied by the displacement ventilation system. As shown in Figure 8 (left), the air supplied by DV was moving at the lower part of the room in two semi-circular flow patterns that met at the center of the wall facing DV, where the source of N_2O is located. This pulled N_2O molecules toward the center of the room where the intake of DPV is located. Therefore, DPV increased the concentration of N_2O in the breathing zone as it was transporting N_2O from the floor to the breathing zone (Figure 8, right).

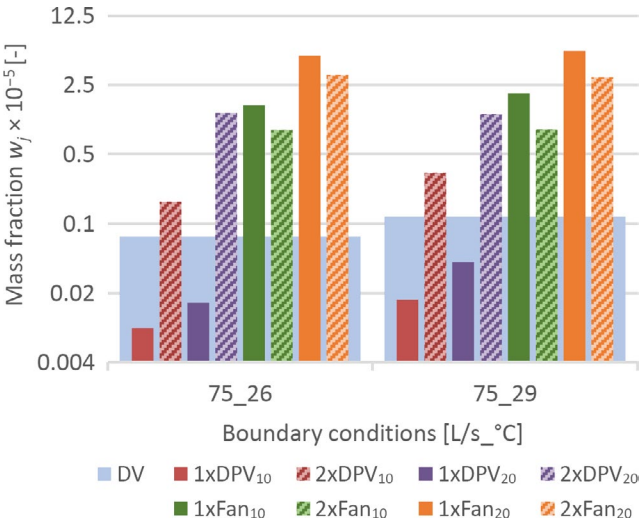

FIGURE 7 SF_6 mass fraction inhaled by the exposed occupant

As shown in Figure 9, when the DPV systems were switched on at both workstations, the inhaled N_2O mass fraction at the exposed workstation was mass fraction was between 5.7×10^{-5} and 6.9×10^{-5}. The amount of N_2O gas transported to the breathing zone through natural convection during the DV reference cases was slightly higher when the room air temperature was cooler ($\theta_{set\text{-}point} = 26°C$). This was caused by a higher air velocity in the microenvironment surrounding the occupants during the cases with the lower room air temperature set point.[48]

All $2xDPV_{10}$ cases increased the inhaled N_2O mass fraction in the exposed workstation compared to the reference DV cases. A room ventilation flow rate of $\dot{V}_{DV} = 60$ L/s yielded a lower inhaled N_2O concentration during the $2xDPV_{10}$ cases compared to the $\dot{V}_{DV} = 75$ L/s cases since the supplied momentum was low at the floor level during the $\dot{V}_{DV} = 60$ L/s cases, ergo less N_2O molecules were pulled to the center of the room where the DPV intakes are located. Conversely, during the cases in which DV ventilation flow rate was set to $\dot{V}_{DV} = 75$ L/s, the high momentum on the floor level pulled more N_2O gas toward the DPV intake resulting in a higher inhaled N_2O mass fraction. Increasing the flow rate of DPV to $\dot{V}_{DPV} = 20$ L/s (ie, DPV_{20} cases) improved the performance compared to the DPV_{10} cases since the air momentum at the DPV intake was high enough to suck the air from a thicker air layer at the lower part of the room. In this layer, N_2O concentration was high in the lower part and low in the upper part. Thus, the sucked air at the DPV intake was a mixture of low-N_2O-concentration air and high-N_2O-concentration air. On average, when switching from $2xDPV_{10}$ to $2xDPV_{20}$, the inhaled N_2O concentration dropped by 37.9%.

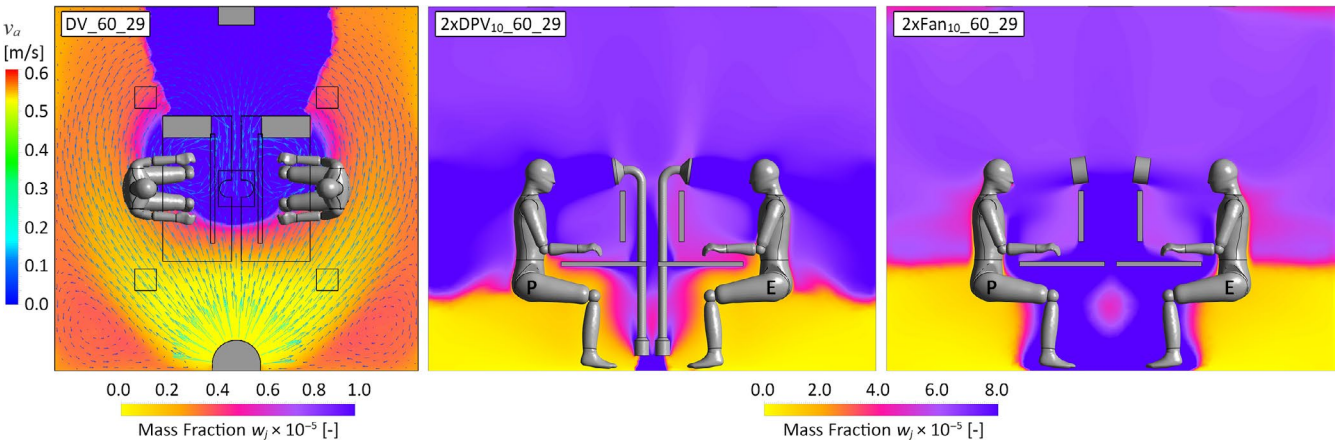

FIGURE 8 Left: velocity vectors and N_2O mass fraction 10 cm above the floor during the DV_60_26 case. Middle and Right: N_2O mass fraction during the $2xDPV_{10}$_60_29 and $2xFan_{10}$_60_29 cases

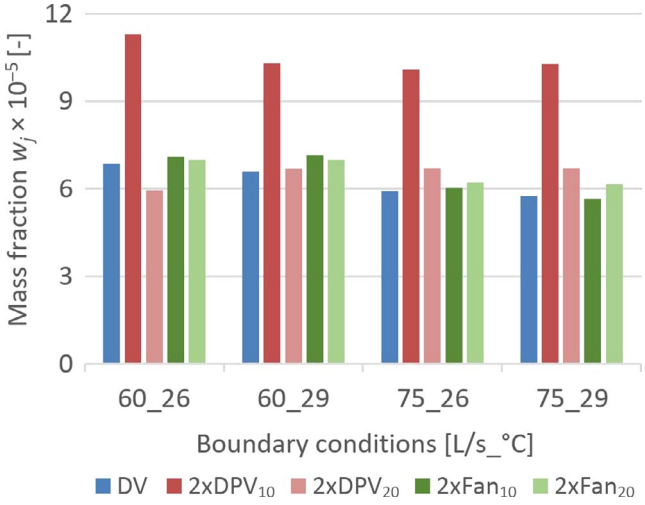

FIGURE 9 N_2O mass fraction inhaled by the exposed occupant. DPV and the fan are switched on at both workstations

Unlike the removal of exhaled contaminants (marked with SF_6), both Fan_{10} and Fan_{20} cases achieved a better inhaled N_2O concentration at the exposed workstation compared to DPV cases. As shown in Figure 8, during the desk fan cases, the thermal plumes from the heat sources at the center of the room were transporting N_2O gas upward through the space between the two desks. Some of these N_2O molecules were redirected by the fan toward the breathing zones of the occupants. The $2xFan_{20}$ cases achieved slightly better results than the $2xFan_{10}$ cases (Figure 9) since the Fan_{20} system was transporting a larger amount of room air compared to the amount of transported N_2O toward the occupants. Both $2xFan_{10}$ and $2xFan_{20}$ cases resulted in nearly similar values of inhaled N_2O concentration as the DV reference cases. When DPV at the polluting workstation was switched off, the inhaled air quality at the exposed workstation was improved (Figure 10). This may have resulted because having two DPV intakes at the center sucked more N_2O gas and moved them to the inhalation level in the room compared to having only one DPV intake switched on, which increased the N_2O concentration in the occupied zone during the $2xDPV_{10}$ and $2xDPV_{20}$ cases compared to the $1xDPV_{10}$ and $1xDPV_{20}$ cases. Additionally, as the flow of the second system was directed at the wall behind the polluting occupant and angled downward, it caused air mixing behind the polluting occupant and pulling the N_2O molecules recirculated through the second DPV toward the center of the room, where the workstations are located. Interestingly, the inhaled N_2O concentration during $1xDPV_{20}$ was even lower than that of the DV reference cases since the $1xDPV_{20}$ cases supplied air with a diluted concentration of N_2O due to air mixing at the intake as explained earlier. On the other hand, the desk fan cases illustrated no significant changes in the inhaled N_2O concentration when switching the fan off at the polluting workstation.

The results reported above indicate that the performance of DPV is highly sensitive to the location of the contamination source, namely to the source close to the system intake. Implementing a DPV intake filter as recommend by Dalewski et al[49] can solve this issue and eliminate the inability of DPV in removing contaminants at floor level. Such filter would also reduce the SF_6 concentration moved toward the inhalation zone. Additionally, it would address the problem of dust and other contaminants that may originate from the carpet which can remarkably restrict implementing DPV in real-life applications.

3.2 | The thermal environment

The DV reference cases yielded a typical displacement ventilation thermal environment in which the indoor environment was vertically divided into two zones: the occupied zone and the upper zone. This stratification was a result of the buoyancy forces generated by the heat sources in the domain. The buoyancy forces transport the air, which was supplied into the lower part of the room with a low velocity and low turbulence intensity, into the upper zone where it was removed from the space through the exhaust outlet.[50] During the $\dot{V}_{DV}$ = 75 L/s reference cases, the difference in air temperature between head and ankle level (0.1 and 1.1 m from the floor) was always smaller than 3 K, thus adhering to the recommendations reported in the ASHRAE 55 standard[51] and buildings in Category B (PPD < 10%, −0.5 < PMV < +0.5) in the ISO 7730 standard.[52] Nevertheless, the $\dot{V}_{DV}$ = 60 L/s reference cases achieved a maximum of 3.25 K vertical temperature gradient. Thus, the vertical air temperature difference was slightly above ASHRAE's recommendations, hence achieving the requirements of buildings in Category C (PPD < 15%, −0.7 < PMV < +0.7) in the ISO 7730 standard. Figure 11A illustrates the horizontal air velocity distribution at 10 cm from the floor during the DV_75_29 case. It shows that the "adjacent zone" of the displacement ventilation diffuser, in which air velocity exceeds 0.2 m/s causing draught discomfort,[11] is located far from the workstations. The maximum length of the adjacent zone L_a during the high flow rate cases ($\dot{V}_{DV}$ = 75 L/s cases) was about 10 cm from the inlet air

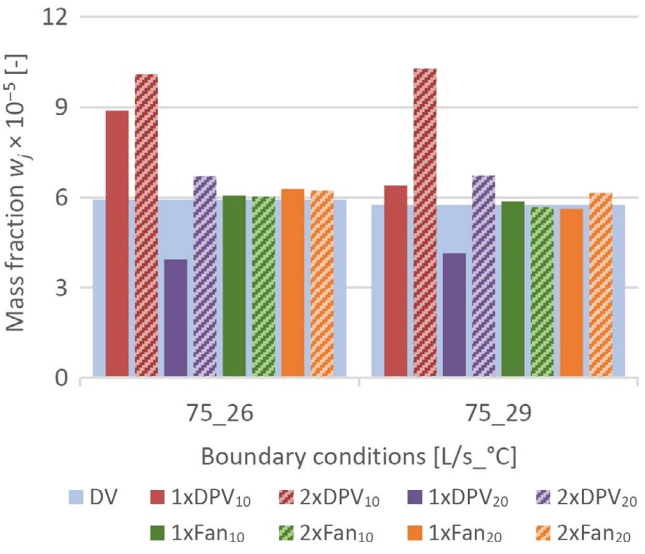

FIGURE 10 N_2O mass fraction inhaled by the exposed occupant

terminal surface. Thus, draught sensation due to elevated velocities at the feet did not occur in any of the simulated cases.

Figure 11B exhibits the vertical air temperature distribution in the space during the 2xDPV$_{20}$ and 2xFan$_{20}$ cases under 60_29 boundary conditions. While DPV was transporting cool air from the floor level into the breathing zone, the fan was moving warm air from the thermal plume above the monitors toward the occupant's face. The dense cool air supplied by DPV mixed completely with the upward DV flow behind the occupants, which destroyed the vertical temperature stratification in that zone. On the other hand, the warm flow from the fan had a lower density than the upward DV flow. Therefore, it could not penetrate all the vertical air layers; instead, it only mixed with the air at the pelvis height. Additionally, DPV altered the flow pattern between the two occupants. As DPV (especially DPV$_{20}$ cases) was taking air from the floor level, the air temperature below the desks and between the monitors was relatively warm. Conversely, the air temperature in these zones was cooler during the fan cases since the cool air supplied by DV slowly moved upward into these zones with no interruption.

Besides altering the temperature distribution in the room, DPV and the fan destroyed the convective boundary layer around the head and disturbed the convective flow around the upper body segments. As illustrated in Figure 11C, DPV decreased the air temperature at the head, whereas the fan cases increased the air temperature at the head. Since the heat emitted by the fan at the DPV intake was not simulated in this study, DPV air temperature was more or less equal to the air temperature at the floor level, which was 1.63-3.25 K lower than the room air temperature. On the other hand, since the fan was located above the screens, the air the fan moved was 1.63-2.27 K warmer than room temperature.

Figure 12 shows that the DPV$_{10}$ and Fan$_{10}$ cases resulted in a cooler inhaled air in comparison with the DPV$_{20}$ and Fan$_{20}$ cases, respectively. This has resulted from higher mixing of cool and warm air at the DPV$_{20}$ intake during the DPV cases and higher suction of the warm air in the ascending thermal plume above the computer monitors during the Fan$_{20}$ cases. DPV$_{10}$ decreased the inhaled air temperature by up to 2.84 K during the 2xDPV$_{10}$_60_26 case compared to the DV_60_26 case, while DPV$_{20}$ lowered the air temperature at the face by a maximum of 2.34 K under the same boundary conditions. The 60_26 boundary conditions achieved the best temperature reduction at the face due to the relatively larger difference in air temperature between head and ankles level, which led to cooler DPV supplied air. During the desk fan cases, however, air temperature around the head was higher than the reference cases by a maximum of 1.84 K and 2.13 K during the Fan$_{10}$ and Fan$_{20}$ cases, respectively. Minimum increase in the inhaled air temperature was 1.37 K during the 2xFan$_{10}$_75_29 case as the thermal plume above the computer monitors was not as strong due to the smaller difference between the monitors' surface temperature and the surrounding room air temperature.

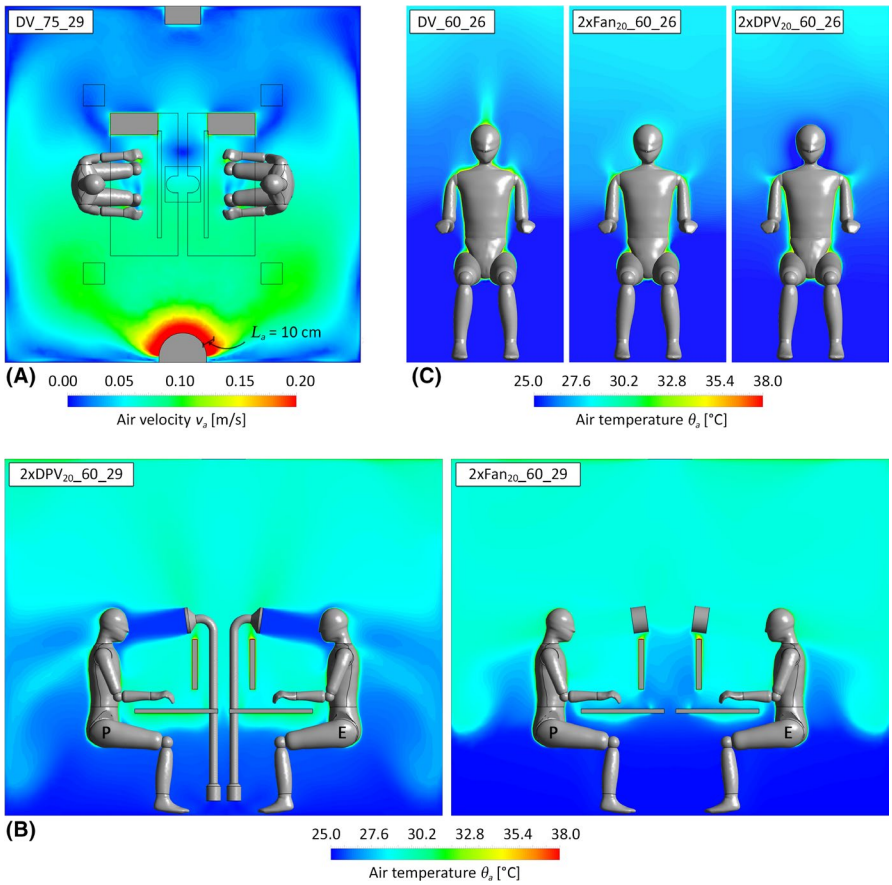

FIGURE 11 (A) Horizontal air velocity distribution 10 cm above the floor during the reference case DV_75_29 case; (B) vertical air temperature gradient during the 2xDPV$_{20}$_60_29 and 2xFan$_{20}$_60_29 cases; and (C) air temperature around the exposed occupant during the 60_26 cases

3.3 | Thermal sensation and comfort

The properties of the thermal environment presented in the previous section were translated into predicted thermal sensation and thermal comfort votes using the coupling of CFD and UCB model. As mentioned in Section 2.4, the UCB model estimates the overall and local thermal response according to Zhang's model, which implements a 9-point scale to evaluate thermal sensation, in which 4 = very hot, 0 = neutral, and − 4 = very cold. To assess thermal comfort, Zhang's model utilizes a different 9-point scale which ranges both upward (where 0 = just comfortable, 4 = very comfortable) and downward (where − 0 = just uncomfortable, −4 = very uncomfortable).[26]

Figure 13 presents the overall thermal sensation S_o and comfort C_o of the exposed occupant during the simulated cases when the personalized system was switched on at both workstations. The colored scale above the graphs indicates the two sides of the thermal sensation and comfort scales. Figure 13 (left) shows that all cases resulted in an overall sensation on the warm side of the sensation scale. The overall sensation during the reference cases with the room set-point temperature of $\theta_{set\text{-}point}$ = 26°C was close to thermal neutrality (0.17 and 0.28 during the DV_60_26 and DV_75_26, respectively). Therefore, the added personalized systems had a minor impact on these cases. Even though the fans moved warm air toward the face, they slightly improved the overall sensation by up to 0.11 during the 2xFan$_{10}$_75_26 case due to elevated target air velocity. The Fan$_{10}$ cases performed slightly better than the Fan$_{20}$ case since the latter supplied air with a higher air temperature as shown in Figure 12. The DPV$_{10}$ and DPV$_{20}$ cases, however, resulted in a slight increase in the overall sensation which can be attributed to disturbing the convective boundary layer and pushing the warm air around the body downward to the forearms and the pelvis region (Figure 11B). Yet, the maximum increase in these cases is still fairly slight (0.08 during the 2xDPV$_{20}$_60_26 case).

However, the cases with the room set-point temperature of $\theta_{set\text{-}point}$ = 29°C exhibited a significant impact of DPV on sensation and improving overall sensation by up to 0.61 points on the thermal sensation scale (during the 2xDPV$_{10}$_60_29 case). Yet, even with the improvement that DPV triggered, the overall thermal sensation during the $\theta_{set\text{-}point}$ = 29°C cases was always above + 1 (corresponding to a "slightly warm" sensation). The fan cases exhibited a different pattern during the $\theta_{set\text{-}point}$ = 29°C cases. In these cases, the Fan$_{20}$ was able to improve thermal sensation by 0.53 points by increasing air velocity at the face to v_a = 0.54 m/s. Fan$_{10}$ cases, however, impaired the overall sensation at the higher ambient temperature set point as it was delivering warm air with low velocity into the breathing zone. Therefore, the Fan$_{10}$ cases resulted in an overall sensation above + 2, corresponding to a thermal sensation vote of "warm."

The overall thermal comfort results exhibited fairly similar patterns to those of the thermal sensation. While the DPV and the fan had a small effect on the overall thermal sensation when $\theta_{set\text{-}point}$ = 26°C, they positively affected the overall thermal comfort. As seen in Figure 13 (right), both DV_60_26 and DV_75_26 achieved a comfort level lower than + 1; yet when the personalized systems were implemented, the overall comfort reached a maximum of 1.77 during the 2xFan$_{10}$_60_26 case. The DPV$_{10}$ and Fan$_{10}$ cases achieved slightly better results compared to DPV$_{20}$ and Fan$_{20}$, respectively. This was caused by potential draft sensation and eye irritation attributed to elevated velocities at the face. However, the DPV$_{20}$ and Fan$_{10}$ still achieved better results in comparison with the DV reference cases. When the ambient air temperature was set to $\theta_{set\text{-}point}$ = 29°C, the DPV$_{10}$ cases had a clear superiority over the Fan$_{10}$

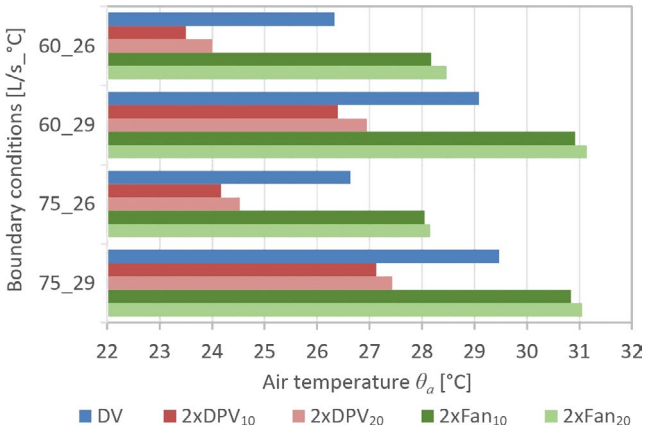

FIGURE 12 Air temperature inhaled by the exposed occupant

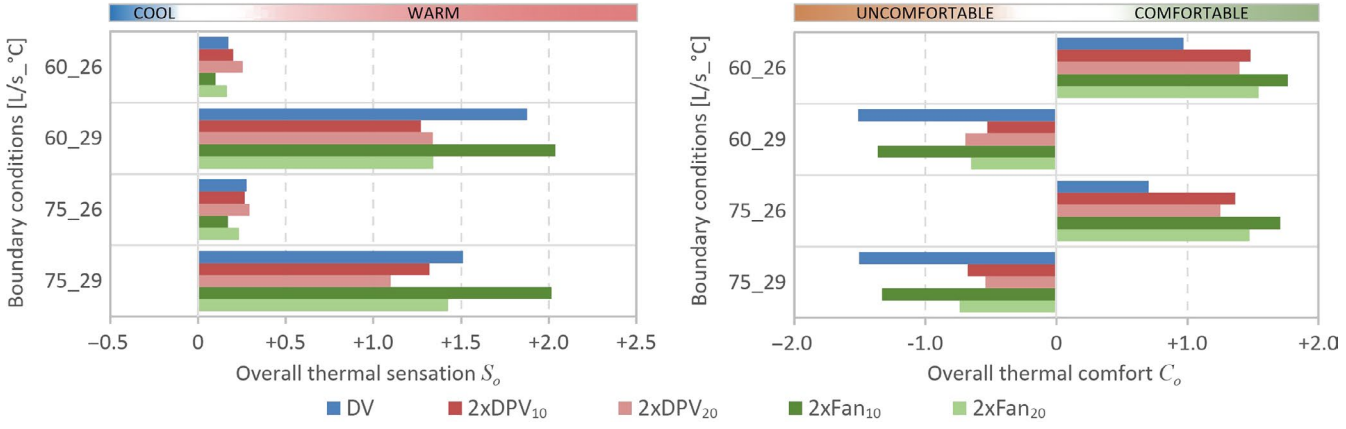

FIGURE 13 The exposed occupant's overall thermal sensation (left) and thermal comfort (right)

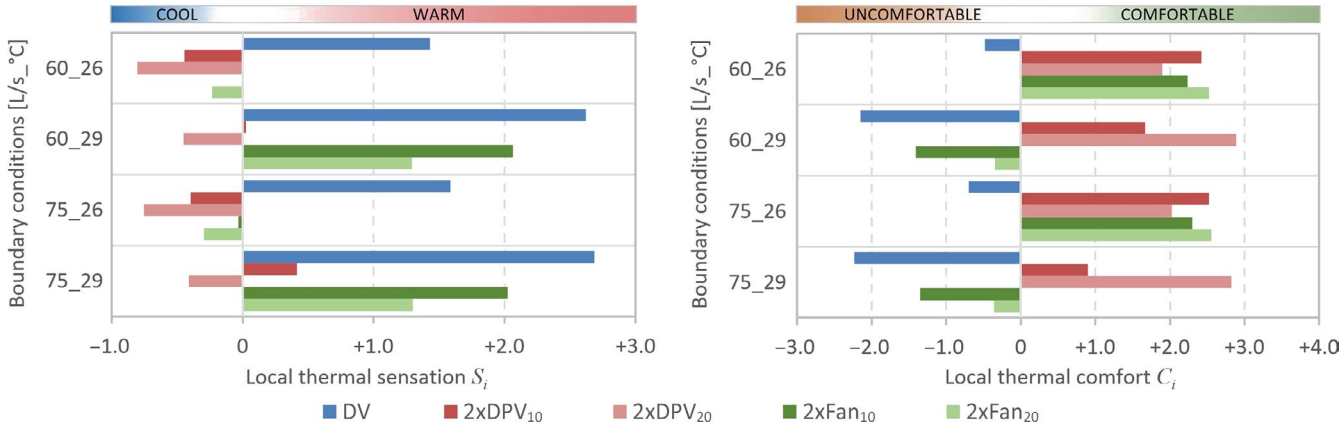

FIGURE 14 The exposed occupant's local thermal sensation (left) and local thermal comfort (right) at the head

cases. The DPV_{10} cases improved overall comfort by up to 0.98 in comparison with the reference case, whereas the maximum overall comfort improvement achieved by Fan_{10} was 0.18 in comparison with the reference case. On the other hand, the Fan_{20} cases achieved comparable overall comfort levels to the DPV_{20} cases. Yet, although the personalized systems improved the overall comfort levels when $\theta_{set\text{-}point}$ = 29°C, the overall comfort values still extended on the "discomfort" side of the comfort scale (C_O < 0) due to the high room air temperature.

Compared to the overall thermal sensation and comfort, DPV and the fan had a larger impact on the local thermal state of the head. As exhibited in Figure 14 (left), during the $\theta_{set\text{-}point}$ = 26°C cases, the reference cases achieved an average thermal sensation of + 1.51 (halfway between "slightly warm" and "warm" sensation). Yet, when DPV was implemented, it shifted the local sensation to the cool side of the sensation scale (S_i < 0), achieving an average of −0.42 and −0.78 during the DPV_{10} and DPV_{20} cases, respectively; that is, achieving a local sensation between "neutral" and "slightly cool" sensation. The fan cases achieved local thermal neutrality as well during the $\theta_{set\text{-}point}$ = 26°C cases. Fan_{20} cases extended local sensation toward "slightly cool," while Fan_{10} cases resulted in mainly "neutral" local sensation due to the difference in local air velocities. Nevertheless, during the $\theta_{set\text{-}point}$ = 29°C cases, the fan cases were not able to pull the head's sensation to neutral because the head's sensation during the 29°C reference cases (DV_60_29 and DV_75_29) was as high as + 2.69. When Fan_{10} was implemented, local sensation dropped to an average of + 2.04 ("warm" sensation), whereas the high-velocity Fan_{20} cases achieved an average of + 1.3. On the other hand, DPV_{20} cases were providing cool air at high velocity, which shifted the head's sensation to the cool side (the negative side) of the scale even when the ambient air temperature was 29°C. DPV_{10} cases, however, kept the local sensation on the warm side of the scale. Yet, the highest achieved local sensation in the DPV_{10} cases was + 0.4 (during the $2xDPV_{10}$_75_29 case), which is fairly close to "neutral" sensation.

The local thermal comfort results shown in Figure 14 (right) correspond to the local thermal sensation results. The $\theta_{set\text{-}point}$ = 26°C reference cases resulted in an average of −0.59 (slightly uncomfortable). When DPV and fans were implemented, they shifted the head's comfort to the "comfortable" side of the comfort scale (C_O > 0), achieving a maximum of + 2.55 points. Interestingly, at $\theta_{set\text{-}point}$ = 26°C, the low-velocity system (DPV_{10}) achieved a better local comfort than the high-velocity system (DPV_{20}). Conversely, the Fan_{20} system performed better than the Fan_{10} system under the same boundary conditions. This indicates that the DPV_{20} combination of cool air and high velocity is less preferred than combining warm air and high velocity. Increasing the room air temperature to $\theta_{set\text{-}point}$ = 29°C yielded a different pattern. In these cases, only DPV was able to shift comfort to the "comfortable" side of the comfort scale. DPV_{20} achieved the best results with a comfort vote as high as + 2.89 during the $2xDPV_{20}$_60_29 case. This indicates that higher velocities at the face are preferred under a warm indoor environment. Consequently, even though the Fan_{20} cases were delivering warm air to the face, they were able to pull the comfort vote close to the "just uncomfortable" vote (close to C_i = 0). By providing warm air at low velocity, the $\theta_{set\text{-}point}$ = 29°C Fan_{10} cases achieved the lowest local comfort values, which, however, still improved local comfort compared to the reference cases.

The results reported in Sections 3.1, 3.2 and 3.3 indicate that besides the location of the contamination source, the location of thermal plumes impacted the performance difference between DPV and the fan. In the simulated office setup, the fan was placed above the computer screens to be in the same location as the DPV diffuser to allow for direct comparison. This considerably impacted the comfort simulation results of the fan as it was moving the warm air from the screen's thermal plume toward the face. Moreover, the thermal plumes above the screens were carrying contaminant from the occupied zone upward toward the exhaust outlet. Hence, placing the fan above the screen impaired the quality of the air that was being moved into the breathing zone. As a result, placing the fan away from the heat sources is recommended to achieve a better performance.

4 | CONCLUSIONS

Both DPV and desk fans are personalized systems that are independent of the central heating, ventilation, and air conditioning (HVAC)

system. They allow the users to personalize their indoor environment according to their individual preferences without restraining the flexibility of the room layout. The conducted CFD simulations showed that when the systems were switched on at both workstations, they both increased the inhaled concentration of SF_6 at the exposed workstation; that is, they both reduced indoor air quality when contrasted to the reference cases. However, when comparing the performance of DPV and desk fans, the fan cases resulted in a higher concentration of inhaled SF_6. When the DPV or the fan at the polluting occupant's workstation was switched off, the spread of exhaled contaminants is mitigated significantly. In these cases, the desk fan scenarios increased the inhaled SF_6 concentration, while the DPV scenarios decreased SF_6 inhaled concentration compared to the reference cases. DPV cases reduced the inhaled SF_6 concentration by as much as 8 times smaller than what it was during the corresponding reference case. On the other hand, the desk fan performed better than DPV in removing the contaminants from a passive source at the breathing zone of the exposed occupant in most cases since the contamination source was located near the DPV intakes. The inability of DPV in removing contaminants emitted on the floor level confirms the necessity of a DPV intake filter.

Thermal comfort simulations illustrated that DPV was preferable to the fan in improving the local thermal sensation and comfort of the head, especially at high ambient air temperatures. Simulations showed that only the DPV cases shifted the local comfort to the comfortable side of the scale (above zero) at 29°C room temperature, whereas the reference cases and desk fan cases resulted in a negative (ie, uncomfortable) values of the head's local comfort under the same boundary conditions. DPV performed better than the desk fans in improving the overall thermal sensation and comfort at 29°C. However, the impact of systems on the overall thermal state was fairly comparable under a 26°C ambient air temperature. Yet, in reality, fans supply air with a much higher turbulence intensity, which was not simulated in this study. As a result, the fan's thermal comfort results would be even lower as occupants prefer flows with low turbulence to avoid draft sensation.

By considering the different aspects of the performance of DPV and a fan, it is evident that DPV is the better option. DPV is, in fact, nothing but a sophisticated, modified desk fan that is equipped with a low-turbulence diffuser, an intake filter, and a pipe to transport air from the lower part of the room. Thus, by implementing these modifications, the performance of the system is remarkably improved without significant increases in its cost.

ACKNOWLEDGEMENTS

This work was supported by a scholarship from the Deutscher Akademischer Austaushdienst (DAAD) (program ID: 57129429). Their constant support is highly appreciated. I would also like to thank Prof. Arsen Melikov for his insightful thoughts and recommendations regarding this project during my short research visit at the Technical University of Denmark. Additionally, we would like to thank the Centre for the Built Environment at the University of California, Berkeley, for their cooperation and for facilitating the use of their comfort model. Additionally, special thanks to the Institute of Structural Mechanics (ISM) at the Bauhaus-Universität Weimar for providing the computational resources needed for conducting this study.

AUTHOR CONTRIBUTION

Hayder Alsaad: Conceptualization (lead); Data curation (lead); Formal analysis (lead); Funding acquisition (lead); Methodology (lead); Project administration (lead); Validation (lead); Writing-original draft (lead); Writing-review & editing (lead). **Conrad Voelker:** Funding acquisition (supporting); Project administration (supporting); Supervision (lead); Writing-original draft (supporting); Writing-review & editing (supporting).

ORCID

Hayder Alsaad https://orcid.org/0000-0001-7738-0193
Conrad Voelker https://orcid.org/0000-0002-3687-0177

REFERENCES

1. Melikov AK. Personalized ventilation. *Indoor Air*. 2004;14:157-167.
2. Tsushima S, Wargocki P, Tanabe S. Sensory evaluation and chemical analysis of exhaled and dermally emitted bioeffluents. *Indoor Air*. 2018;28:146-163.
3. Wolkoff P. Indoor air humidity, air quality, and health - An overview. *Int J Hyg Environ Health*. 2018;221:376-390.
4. Bakó-Biró Z, Wargocki P, Weschler CJ, Fanger PO. Effects of pollution from personal computers on perceived air quality, SBS symptoms and productivity in offices. *Indoor Air*. 2004;14:178-187.
5. Lagercrantz L, Wistrand M, Willen U, Wargoski P, Witterseh T, Sundell J. Negative impact of air pollution on productivity: Previous Danish findings repeated in new Swedish test room. Proceedings of Healthy Buildings 2000, Helsinki. 2000;1:653–658.
6. Wargocki P, Wyon DP, Sundell JA, Clausen GE, Fanger PO. The effects of outdoor air supply rate in an office on perceived air quality, sick building syndrome (SBS) symptoms and productivity. *Indoor Air*. 2000;10:222-236.
7. Fanger P. Human requirements in future air-conditioned environments. *Int J Refrig*. 2001;24:148-153.
8. Chludzińska M, Bogdan A. The effect of temperature and direction of airflow from the personalised ventilation on occupants' thermal sensations in office areas. *Build Environ*. 2015;85:277-286.
9. Melikov AK, Cermak R, Majer M. Personalized ventilation: evaluation of different air terminal devices. *Energy Build*. 2002;34:829-836.
10. Dalewski M, Melikov AK, Vesely M. Performance of ductless personalized ventilation in conjunction with displacement ventilation: Physical environment and human response. *Build Environ*. 2014;81:354-364.
11. Skistad H, Mundt E. Displacement ventilation in non-industrial premises. Brussels: REHVA, Federation of European Heating and Air-conditioning Associations; 2002.
12. Dalewski M, Veselý M, Melikov AK. Human response to ductless personalized ventilation coupled with displacement ventilation. Proceedings of Healthy Buildings 2012, Brisbane, Australia. 2012;1.
13. Halvonova B, Melikov A. Performance of ductless personalized ventilation in conjunction with displacement ventilation: Impact of workstations layout and partitions. *HVAC R Res*. 2010;16:75-94.
14. Halvoňová B, Melikov AK. Performance of "ductless" personalized ventilation in conjunction with displacement ventilation: Impact of disturbances due to walking person(s). *Build Environ*. 2010;45:427-436.

15. de Dear RJ, Akimoto T, Arens EA, et al. Progress in thermal comfort research over the last twenty years. *Indoor Air*. 2013;23:442-461.
16. Alsaad H, Voelker C. Qualitative evaluation of the flow supplied by personalized ventilation using schlieren imaging and thermography. *Build Environ*. 2020;167:106450.
17. Rohles FHJ, Woods JE, Nevins RG. Effects of air movement and temperature on the thermal sensations of sedentary man. *ASHRAE Transact*. 1974;80:101-119.
18. Scheatzle D, Wu H, Yellott J. Expanding the summer comfort envelope with ceiling fans in hot, arid climates. *ASHRAE Transact*. 1989;95:269-280.
19. Arens E, Xu T, Miura K, Hui Z, Fountain M, Bauman F. A study of occupant cooling by personally controlled air movement. *Energy Build*. 1998;27:45-59.
20. Yang B, Schiavon S, Sekhar C, Cheong D, Tham KW, Nazaroff WW. Cooling efficiency of a brushless direct current stand fan. *Build Environ*. 2015;85:196-204.
21. Schiavon S, Yang B, Donner Y, Chang VW-C, Nazaroff WW. Thermal comfort, perceived air quality, and cognitive performance when personally controlled air movement is used by tropically acclimatized persons. *Indoor Air*. 2017;27:690-702.
22. Zhai Y, Zhang Y, Zhang H, Pasut W, Arens E, Meng Q. Human comfort and perceived air quality in warm and humid environments with ceiling fans. *Build Environ*. 2015;90:178-185.
23. Nielsen PV. Fifty years of CFD for room air distribution. *Build Environ*. 2015;91:78-90.
24. Alsaad H, Voelker C. Performance assessment of a ductless personalized ventilation system using a validated CFD model. *J Build Perform Simul*. 2018;11:689-704.
25. Huizenga C, Zhang H, Arens E. A model of human physiology and comfort for assessing complex thermal environments. *Build Environ*. 2001;36:691-699.
26. Zhang H. Human thermal sensation and comfort in transient and non-uniform thermal environment: Center for the Built Environment, University of California, Berkeley; 2003.
27. ASHRAE. *ASHRAE Handbook: Fundamentals*. Atlanta, GA: American Society of Heating, Refrigeration and Air-Conditioning Engineers; 2017.
28. Bolashikov Z, Nikolaev L, Melikov AK, Kaczmarczyk J, Fanger PO. New air terminal devices with high efficiency for personalized ventilation application. Proceedings of Healthy Buildings 2003, Singapore. 2003;2:850-855.
29. Hyldgård CE. Humans as a source of heat and air pollution. Proceedings of ROOMVENT '94, Fourth International Conference on Air Distribution in Rooms, Cracow, Poland. 1994;1:413-433
30. Gupta JK, Lin C-H, Chen Q. Characterizing exhaled airflow from breathing and talking. *Indoor Air*. 2010;20:31-39.
31. Pantelic J, Sze-To GN, Tham KW, Chao CYH, Khoo YCM. Personalized ventilation as a control measure for airborne transmissible disease spread. *J R Soc Interface*. 2009;6(Suppl 6):S715-S726.
32. Höppe P. Temperatures of expired air under varying climatic conditions. *Int J Biometeorol*. 1981;25:127-132.
33. Melikov AK. Human body micro-environment: The benefits of controlling airflow interaction. *Build Environ*. 2015;91:70-77.
34. Tang JW, Noakes CJ, Nielsen PV, et al. Observing and quantifying airflows in the infection control of aerosol- and airborne-transmitted diseases: an overview of approaches. *J Hosp Infect*. 2011;77:213-222.
35. Nielsen PV, Olmedo I, de Adana MR, Grzelecki P, Jensen RL. Airborne cross-infection risk between two people standing in surroundings with a vertical temperature gradient. *HVAC R Res*. 2012;18:552-561.
36. Antoun S, Ghaddar N, Ghali K. Coaxial personalized ventilation system and window performance for human thermal comfort in asymmetrical environment. *Energy Build*. 2016;111:253-266.
37. Hjermann T. CFD simulation of active displacement ventilation [Master thesis]. Norway: Norwegian University of Science and Technology, Department of Energy and Process Engineering; 2017
38. ANSYS. ANSYS® Academic Research, Release 16.2, Help System, Coupled Field Analysis Guide. 2015. www.ansys.com.
39. Chen Q, Glicksman L. *System Performance Evaluation And Design Guidelines For Displacement Ventilation*. Atlanta, GA: American Society of Heating, Refrigerating, and Air-Conditioning Engineers, Incorporated; 2003.
40. EN15251. Criteria for indoor environment including thermal, indoor air quality, light and noise. Brussels: European Committee for Standardization; 2007.
41. Kelley CT, Keyes DE. Convergence analysis of pseudo-transient continuation. *SIAM J Numer Anal*. 1998;35:508-523.
42. Zhu S, Cai W, Spengler JD. Control of sleep environment of an infant by wide-cover type personalized ventilation. *Energy Build*. 2016;129:69-80.
43. Russo JS, Khalifa HE. CFD assessment of intake fraction in the indoor environment. *Build Environ*. 2010;45:1968-1975.
44. Fanger P. Calculation of thermal comfort: Introduction of a basic comfort equation. *ASHRAE Transact*. 1967;73:III.4.1-III.4.20.
45. Stolwijk J. A mathematical model of physiological temperature regulation in man. Washington, D.C.: NASA Contractor Reports CR-1855; 1971.
46. Voelker C, Alsaad H. Simulating the human body's microclimate using automatic coupling of CFD and an advanced thermoregulation model. *Indoor Air*. 2018;28:415-425.
47. Fanger O. What is IAQ? *Indoor Air*. 2006;16:328-334.
48. Voelker C, Maempel S, Kornadt O. Measuring the human body's microclimate using a thermal manikin. *Indoor Air*. 2014;24:567-579.
49. Dalewski M, Vesely M, Melikov AK. Ductless personalized ventilation with local air cleaning. 10th International Conference on Healthy Buildings 2012, Brisbane, Australia. 2012;1.
50. Abbas T. Displacement ventilation and static cooling devices: Building Services Research and Information Association; 1999.
51. ASHRAE. ANSI/ASHRAE Standard 55: Thermal environmental conditions for human occupancy. Atlanta, GA: American Society of Heating, Refrigeration and Air Conditioning Engineers, Inc; 2013.
52. ISO 7730. Ergonomics of the thermal environment — Analytical determination and interpretation of thermal comfort using calculation of the PMV and PPD indices and local thermal comfort criteria. Geneva, Switzerland: International Organization for Standardization; 2005.

How to cite this article: Alsaad H, Voelker C. Performance evaluation of ductless personalized ventilation in comparison with desk fans using numerical simulations. *Indoor Air*. 2020;00:1–14. https://doi.org/10.1111/ina.12672